Marker Displacement Measurements of Polymer–Polymer Interdiffusion†

Peter F. Green, Christopher J. Palmstrøm, James W. Mayer, and Edward J. Kramer*

Department of Materials Science and Engineering and the Materials Science Center, Cornell University, Ithaca, New York 14853. *Received April 27, 1984*

ABSTRACT: Interdiffusion of two polymer species with very different molecular weights, and thus very different self-diffusion coefficients D^*, should lead to a net flux of matter and displacement Δx_m of inert markers placed at the original interface of the couple. Theory predicts that $\Delta x_m = C(D^*_A t)^{0.5}$ where A is the faster diffusing (lower molecular weight) species and C depends only weakly on the ratio of molecular weights as long as these are quite different. This analysis is used to measure the D^*_A of monodisperse polystyrenes (PS) which vary in molecular weight M from 33 000 to 943 000. Polystyrene films of molecular weight M are placed on a thick PS film substrate of higher molecular weight, $M_B = 2 \times 10^7$ or 1.8×10^6, the surface of which had been "decorated" with small gold particles by vacuum evaporation of gold. The displacement Δx_m of the Au markers toward the surface of the interdiffusing film sandwich is monitored by Rutherford backscattering spectrometry and is found to increase as $t^{0.5}$ as expected, where t is the diffusion time at 174 °C. As predicted by the reptation theory, D^*_A is found to decrease as M^{-2} and its magnitude is close to both the prediction of that theory and to the values measured by other methods.

Introduction

The way in which entanglements affect the dynamical properties of concentrated melts of long-chain polymeric molecules is of great current interest.[1-3] The theory of reptation proposed by de Gennes,[4] though constructed to describe the one-dimensional translational motion of a chain in the presence of fixed obstacles, adequately describes that of a chain in a concentrated melt. This theory considers a chain of N monomers and total molecular mass M. This chain which has a random coil conformation is trapped in an environment of fixed obstacles, none of which it is allowed to cross. The chain can undergo one-dimensional translational motion by the propagation of kinks along its length, as illustrated in Figure 1.

The time t_R required for the chain to lose all memory of its original conformation by reptation increases as M^3. Since the mean square displacement of the center of mass of the chain at t_R increases as M, the diffusion coefficient D^* of the chain in the array of obstacles decreases as M^{-2}. It was later pointed out by Edwards[5] that the topological constraints imposed by the neighboring molecules in the melt can be considered to form a virtual tube of length $L = l/(N_e)^{0.5}$ where l is the contour length of the chain and N_e is the number of mers per entanglement length. Klein[6] showed that these constraints would only relax after a tube renewal time t_r which increases as M^5, where M is the molecular mass of the chains surrounding the diffusing chain. For a melt of monodisperse chains where $M \gg M_e$, the entanglement molecular mass, Klein's result implies that $t_R \ll t_r$. Thus the constraints are essentially fixed for the time t_R required for the diffusion of a molecule out of its tube and the result of reptation theory for D^* should accurately give D^* for self-diffusion of entangled chains in the melt.

There have been some previous experiments performed to measure the molecular weight dependence of D^*. Evidence for reptation in polydisperse polyethylene melts has been obtained by Klein[7] and by Klein and Briscoe.[8] They performed experiments in which very dilute concentrations of deuterated polyethylene (DPE) were allowed to diffuse into a PE matrix. The broadening of the initial step function concentration profile of the labelled molecules was monitored by using infrared microdensitometry. The diffusion coefficient extracted from these profiles decreased as $M_w^{-2.0\pm0.1}$ where M_w is the weight-average molecular weight. However only polydisperse ($M_w/M_n \simeq 2$) DPE's were available to Klein and only relatively large D^*'s could be measured due to the limited spatial resolution ($\simeq 100$ μm) of the IR microdensitometry technique. (Klein's recent measurements[9] on deuterated polybutadienes were made on monodisperse material, however.)

A different, and higher resolution, method was pioneered by Smith and co-workers.[10] They labeled the center of poly(propylene oxide) molecules with fluorescent probes, whose fluorescence could be permanently destroyed photochemically by high-intensity light of certain wavelengths. By first bleaching a grating produced by interference of two beams of high-intensity laser light onto the sample and then monitoring the return of the fluorescence signal produced by a low intensity "probe" grating, they were able to determine the diffusion coefficient of the dilute labeled chains in a poly(propylene oxide) matrix of different molecular weight. They found that D^* of the probe molecules increased with decreasing M of the matrix polymer when this molecular weight was not much larger than M_e. This result indicates that the tube renewal must be taken into account in these circumstances. For self-diffusion they find however that D^* scales as M^{-2}. The main experimental difficulty of the technique is the need for sub-micron dimensional stability of the sample (any rigid body translation of the grating will cause a return of fluorescence).

Bartels, Graessley, and Crist[11] have demonstrated yet another method to measure D^*. They produced alternating multilayer films of hydrogenated and deuterated monodisperse polybutadienes and monitored the diffusion mixing of these layers by measuring neutron diffraction from the multilayer sandwich. They found a D^* of 1.4×10^{-11} cm^2/s at 125 °C, a value in good agreement with an extrapolation of the results of Klein and Briscoe.[8] Other techniques such as NMR, forced Rayleigh scattering, and quasi-elastic light scattering have also been used to measure diffusion in polymer systems but are difficult to apply to very slowly diffusing, high molecular weight polymer melts which are the most important test of reptation concepts. The capabilities and results from these methods, as well as the others mentioned previously, have been reviewed recently.[27]

While all of these experiments above have produced results consistent with the reptation theory, most have

† MSC Report No. 5264. Issued by the Materials Science Center.

0024-9297/85/2218-0501$01.50/0

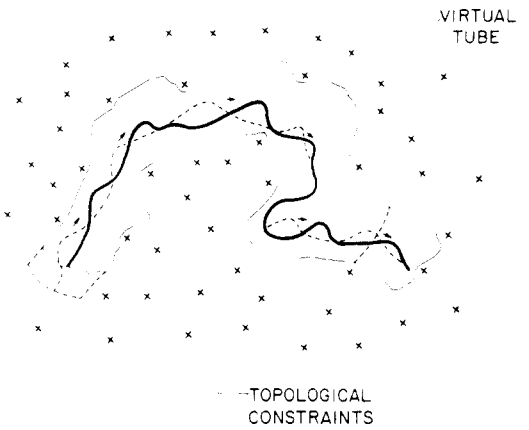

Figure 1. Schematic drawing of a polymer chain diffusing in the melt. The topological constraints of other chains (entanglements) define a virtual tube within which the chain crawls or reptates by propagation of kinks along its length.

followed the diffusion of a dilute polymeric species. Most diffusion problems of practical interest in polymers involve concentrated diffusion couples. Kumagai and co-workers[12] have measured the interdiffusion between a thin layer of monodisperse polystyrene 2–3 μm thick on top of a thick film of monodisperse polystyrene of the same or different molecular weight. The diffusion coefficients extracted showed large deviations from the predicted M^{-2} dependence of reptation. If only their self-diffusion data are examined, i.e., that when M on both sides of the initial interface was the same, the four points fall roughly on a line described by M^{-2}. While other experiments on interdiffusing polymer blends[13] have reported large deviations from the M^{-2} dependence, these probably arise from the large negative enthalpy of mixing typical of these systems.[14] These polystyrene experiments, which cannot have such enthalpies, are the most surprising since the diffusion of a labeled chain is not supposed to be affected by the molecular weight of the polymer surrounding the chain, as long as it is well above M_e.[15]

In this paper we reexamine the interdiffusion in polystyrene thin films. We exploit the excellent depth resolution of Rutherford backscattering spectrometry (RBS) to measure the D^* of monodisperse polystyrene (PS) as a function of M. Small gold "markers" are placed at the interface between an underlying film of ultrahigh molecular mass PS (e.g., 2×10^7) and a top PS film, about 1 μm thick, of lower molecular mass M. Since the lower molecular weight chains diffuse into the ultrahigh molecular weight PS orders of magnitude faster than the ultrahigh molecular weight chains diffuse into the low molecular weight side of the diffusion couple, the gold markers move to the low molecular weight surface of the film sandwich at a rate which reflects the D^* of the faster diffusing (low molecular weight) species.[16] RBS measurements of the gold marker movements in sandwiches with top layers of different M thus allow us to determine both the magnitude of D^* and its dependence on M. The results are in good agreement with the predictions of the reptation theory.

Theory of Polymer Interdiffusion

Consider a slab of glassy polymer A of degree of polymerization N_A welded to the same polymer, B, of degree of polymerization N_B. Now, allow these slabs to interdiffuse at a temperature T, where T is above the glass transition temperature T_g. During this process, in addition to the fluxes of A and B segments J_A and J_B, there is a net matter flux (bulk flow)[17] which may formally be described as a vacancy flux, J_v, which arises for the following reason. As a chain diffuses, it creates portions of a new tube ahead of it and destroys the old as indicated in Figure 1. In the process, a vacant region must be created ahead of the chain into which it can move and when it does so, a vacant region is left behind it. A flux of vacancies results which corresponds to J_v.

Consider the polymer chains to be arranged on a quasi-lattice with each segment of a given polymer chain occupying one site on this "lattice". If "lattice" sites are conserved during interdiffusion then

$$J_A + J_B + J_v = 0 \tag{1}$$

Brochard, Jouffroy, and Levinson,[18] hereafter abbreviated as BJL, assume that $J_v = 0$. This assumption requires a substantial chemical potential gradient $\nabla\mu_v$ (or osmotic pressure gradient, $\nabla\Pi = \nabla\mu_v/\Omega$ where Ω is the volume of a quasi-lattice site) if the molecular weights of A and B are much different.[16] In melts of linear polymers one expects any large gradients of Π to be relaxed quickly so that $\nabla\mu_v = 0$, which is the alternate assumption we propose.[16]

Each of these fluxes can be written in terms of the intrinsic diffusion coefficients D_A and D_B of species A and B, respectively

$$J_A = -D_A\nabla\phi/\Omega \tag{2a}$$

$$J_B = D_B\nabla\phi/\Omega \tag{2b}$$

$$J_v = (D_A - D_B)\nabla\phi/\Omega \tag{2c}$$

where ϕ is the volume fraction of A segments. D_A and D_B are given by

$$D_A = N_A D^*_A[(1 - \phi)/N_A + \phi/N_B] \tag{3a}$$

$$D_B = N_B D^*_B[(1 - \phi)/N_A + \phi/N_B] \tag{3b}$$

The self-diffusion coefficients D^*_A and D^*_B are given by

$$D^*_A = N_e B_0 k_B T/N_A^2 \tag{4a}$$

and

$$D^*_B = N_e B_0 k_B T/N_B^2 \tag{4b}$$

where N_e is the number of monomers in a chain of mass M_e, B_0 is the curvilinear Rouse mobility and k_B is Boltzmann's constant.

Since polymers A and B have unequal intrinsic diffusion coefficients, J_A is not equal to J_B and a net flux of matter will flow across any plane in the "lattice" in the direction of the slower moving species. If inert markers are placed at the initial interface between the two polymers, they should move toward the side of the diffusion couple containing the high concentration of the faster moving species (smaller M). The velocity V of the markers with respect to a coordinate system whose origin is fixed at one end of the diffusion couple is given by[16]

$$V = \Omega J_v = (D_A - D_B)\nabla\phi \tag{5}$$

Substituting in the expressions for D_A and D_B the velocity can be written in terms of the self-diffusion coefficient of species A

$$V = D^*_A\alpha(1 - \alpha\phi)\nabla\phi \tag{6}$$

where $\alpha = 1 - (N_A/N_B)$.

While V of the markers may be determined from experiment, ϕ and $\nabla\phi$ must be known at the location of the markers if D^*_A is to be extracted from the data. One must thus solve the concentration-dependent diffusion equation for the concentration profile of A.

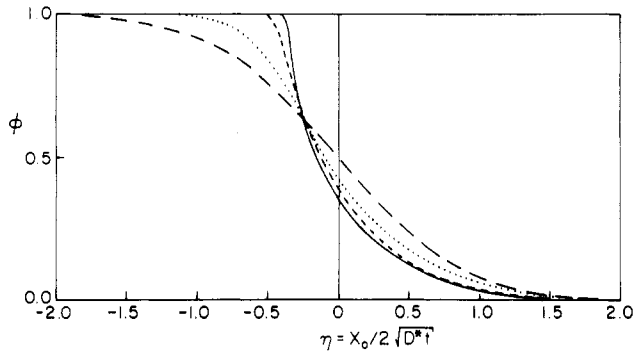

Figure 2. The concentration profile of the lower molecular weight chains (A) diffusing into higher molecular weight chains (B) computed numerically for several molecular weight ratios of A to B. (--) $N_A/N_B = 1$; (···) $N_A/N_B = 0.5$; (- - -) $N_A/N_B = 0.1$; (—) $N_A/N_B = 0.01$.

Consider the inert markers at the initial interface to be at a position x_m relative to the origin of the coordinate system. Now define a second coordinate system x_0 using the markers as its origin so that

$$x = x_0 + x_m \tag{7}$$

Fick's second law can then be written as

$$\frac{\partial \phi}{\partial t} = \frac{\partial}{\partial x}\left(\tilde{D}(\phi)\frac{\partial \phi}{\partial x}\right) \tag{8}$$

where $\tilde{D}(\phi)$ is the concentration-dependent interdiffusion coefficient, which is computed from the intrinsic diffusion coefficents as follows:[16]

$$\tilde{D}(\phi) = (1 - \phi)D_A + \phi D_B = D^*_A(1 - \alpha\phi)^2 \tag{9}$$

Equation 8 can be converted into an ordinary differential equation by use of the Boltzmann transformation

$$\eta = x_0/(4D^*_A t)^{0.5} \tag{10}$$

which yields

$$\frac{1}{2}\eta\frac{d\phi}{d\eta} = \frac{d}{d\eta}\left[(1 - \alpha\phi)^2\frac{d\phi}{d\eta}\right] \tag{11}$$

This differential equation was solved numerically for various values of α by a procedure discussed in Appendix A. The concentration profiles computed for $N_A/N_B = 1$, 0.5, 0.1, and 0.01 are shown in Figure 2. As N_A/N_B becomes much less than 1, the curves approach an asymptotic shape which is quite different from the error function solution obtained when $N_A = N_B$ and D is independent of composition.

By integrating eq 6 the following expression for the displacement of the markers is obtained:

$$\Delta x_m = C(D^*_A t)^{0.5} \tag{12}$$

where

$$C = \phi'(0)\alpha(1 - \alpha\phi(0))$$

The marker displacement should therefore be proportional to $t^{0.5}$ and the slope of a plot of Δx_m vs. $t^{0.5}$ should give $C(D^*_A)^{0.5}$. From the numerical solutions of eq 11, C was determined as a function of N_A/N_B and the results are displayed in Figure 3. As required C goes to 0 as N_A approaches N_B and it approaches a limiting value of 0.48 corresponding to the limiting curve in Figure 2 as $N_A \ll N_B$. Measurements of inert marker displacements can thus be converted using Figure 3 into values of D^*_A for any significantly different N_A and N_B.

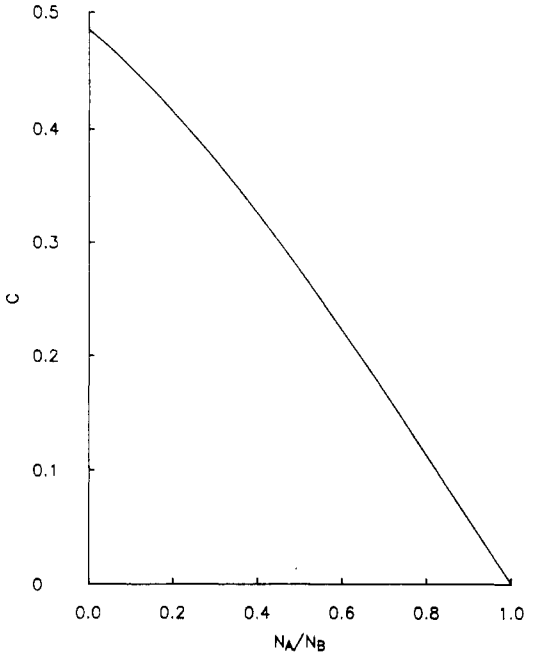

Figure 3. Computed marker displacement factor C vs. the molecular weight ratio of polymer A to polymer B.

Experimental Methods

Silicon wafers, 4 cm^2 in area, were coated with a thin base layer of monodisperse PS ($M_w/M_n < 1.2$) of ultrahigh molecular weight M_B. Base films of $M_w = 2 \times 10^7$ and $M_w = 1.8 \times 10^6$ were cast from polystyrenes purchased from Pressure Chemical Co. The thickness of this base layer was about 2 μm, as measured by optical interference microscopy.

A discontinuous thin film of gold was then evaporated onto the polymer surface under a vacuum of approximately 10^{-5} torr. A transmission electron micrograph showing the initial gold particle size (about 1.8 nm) and interparticle spacing (about 2.5 nm) is shown in Figure 4a. While one might imagine that such small, closely spaced gold particles might block polymer interdiffusion, or at least diffuse rapidly in the viscous polymer melt, neither of these events takes place. Instead, at the diffusion temperature the gold particles coarsen rapidly, forming rafts of much larger particles in the interfacial plane. A typical gold particle distribution in the early stages of an interdiffusion experiment is shown in Figure 4b. These rafts of gold particles form the inert markers on which our method is based.

A second film of monodisperse PS ($M_w/M_n < 1.06$, also from Pressure Chemical Co.) was prepared. The molecular weight of this PS was M, lower than the molecular weight M_B of the base film. This second film was cast by drawing a glass slide at constant rate from a solution of the PS. The film, about 1 μm thick, was floated off the glass slide onto the surface of a bath of distilled water from where it could be picked up on top of the gold decorated base PS layer on the silicon wafer. The final PS sandwich, with the gold markers at the interface, is shown schematically in Figure 5.

The depth of the gold marker below the top surface of the sandwich was measured by Rutherford backscattering spectrometry (RBS). In this technique a beam of He^{2+} ions of energy E_0 (2.14 MeV in our experiments) is directed at the sample at normal incidence as shown in Figure 4. A small fraction of this beam of ions collides elastically with nuclei in the film and is backscattered into an energy-sensitive detector. The He^{2+} ions backscattered at the outer surface have an energy E_1 which is related to their initial energy E_0 by the kinematic factor K_m, i.e.

$$E_1 = K_m E_0 \tag{13}$$

where K_m for a scattering angle of 180° is given by

$$K_m = [(m - m_{He})/(m + m_{He})]^2 \tag{14}$$

and where m and m_{He} are the masses of the target nucleus and He ion, respectively. Ions rebounding from a heavy Au nucleus

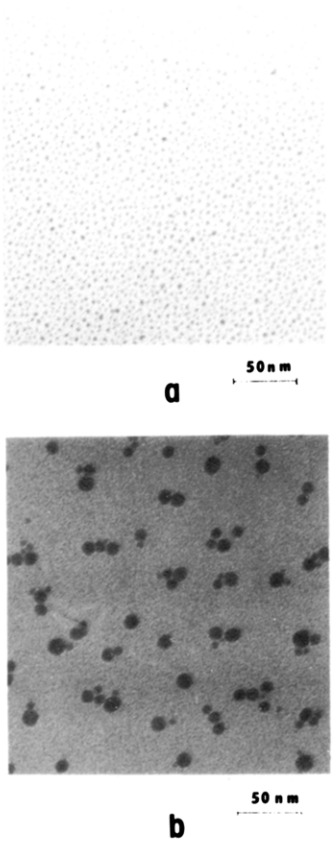

Figure 4. (a) Transmission electron micrograph of the initial gold particle morphology, before diffusion. (b) Coarsened gold particle morphology after 1 h at 174 °C.

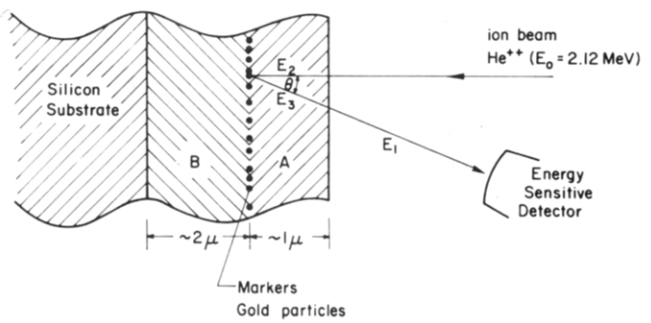

Figure 5. Schematic drawing of the Si wafer/polystyrene/Au/polystyrene sandwich showing the geometry of the Rutherford backscattering experiment.

retain a much larger fraction of their initial energy (K_{Au} = 0.9225) than those scattered by the ligher carbon nucleu (K_C = 0.2526). The hydrogen nuclei in the PS, being of lower mass than He, cannot cause backscattering.

As the beam traverses the sample it loses energy via electronic excitations. Thus if the scattering nucleus lies at a depth x below the surface, the ion loses energy before, and after, the collision as it traverses the film. Whereas Au at the surface of the specimen would produce a peak in the backscattered He ion spectrum at 1.956 MeV for 2.120 MeV incident ion energy, a layer of Au "marker" particles below the surface will produce a peak at an energy that is lower by

$$\Delta E = K_{Au}E_0 - E_1 = [S]x \tag{15}$$

where $[S]$, the energy loss factor, is given by

$$[S] = K_{Au}(dE/dx)_{in} + (1/\cos\theta)(dE/dx)_{out} \tag{16}$$

where $(dE/dx)_{in}$ and $(dE/dx)_{out}$ are the mean energy losses per unit depth of the ion traveling into, and out of, the film, respectively. The energy loss factor $[S]$ may be computed based on the density and the stopping cross-sections of the individual elements in the PS[19] or it can be determined experimentally by measuring the shift of the Au peak to lower energy produced by PS films of known thickness. We find the $[S]^{-1}$ is approximately constant over the depth range of interest at 2.2 nm/keV, or 11 nm/channel on the multichannel analyzer.

Results

Figure 6a shows a typical RBS spectrum from the Si/PS/Au/PS sample prior to interdiffusion. The normalized yield corresponds to $n/(Q\mathcal{E}\Omega)$, where n is the number of ions (counts) in each channel, Q is the total charge of the ions hitting the sample in microcoulombs (1 for this spectrum), $\mathcal{E}$ is the energy width of each channel in keV (4.95 in our case), and Ω is the solid angle subtended by the detector in msr (3.4 in our case). The abrupt rise in yield below channel 110 (E_1 = 0.545 MeV) is due to He ions scattered by carbon nuclei at the surface of the PS film and below. The sharp peak in yield at about channel number 290 (E_1 = 1.436 MeV) is due to He ions scattered from the Au marker particles. This peak occurs at much lower energy than that from Au at the surface (channel number 398, E_1 = 1.956 MeV) due to the energy loss in traversing the overlying PS film.

Each sample was heated to 174 °C under a vacuum of 10^{-3} torr for progressively longer times to allow interdiffusion to occur. After each anneal, the RBS spectrum was measured and the energy of the Au peak noted. The wafer was moved laterally for each analysis so that a fresh area of the PS film sandwich was ion bombarded each time. This precaution is necessary because the ion beam cross-links the PS film and will remove the possibility of any further interdiffusion. Although no shift in the position of the Au peak during acquisition of the spectrum could be measured, indicating negligible loss of C from the overlying PS film as a result of ion damage, the total dose of ions was held to the minimum (1–5 μC) necessary to produce a clearly defined Au peak.

Parts b and c of Figure 6 show the Rutherford backscattering spectra from the sample in Figure 6a after it was annealed at 174 °C for 0.5 and 1.3 h, respectively. After 0.5 h the Au peak has moved to channel number 340 and after 1.3 h it has moved to channel number 378, E_1 = 1.683 and 1.871 MeV, respectively. This sample has a top PS layer with M = 33 000, and a bottom PS layer with M_B = 2×10^7. Since the PS molecules initially in the top layer diffuse into the bottom layer much faster than the much larger molecules in the bottom layer diffuse into the top layer (from the reptation theory the ratio of the D's is almost 10^6), there is a net mass flow past the markers and they move toward the surface. As a consequence, the energy loss of the He ions scattered from the gold markers decreases and the Au peak in the RBS spectrum moves toward higher energies. The peak shifts correspond to marker displacements of 550 and 968 nm, respectively. Note that the Au peak has remained relatively sharp. This observation rules out the possibility that the peak shift is due to an asymmetric Brownian motion of the Au markers themselves due to the very different viscosities of the different molecular weight layers. Such Brownian motion would lead to asymmetric peak broadening, but the peak position itself would remain stationary in energy.

The analysis above, which culminates in eq 12, requires that the marker displacements increase as the square root of the diffusion time. Figure 7 shows a plot of marker displacement vs. $t^{0.5}$ for PS top layers of M = 33 000, 254 000, and 390 000 on a PS bottom layer of $M_B = 2 \times 10^7$. A linear relationship is obtained, the slope of which gives $C(D^*_A)^{0.5}$.

Marker displacement data were obtained from two series of samples. The first series had PS layers with M = 33 000,

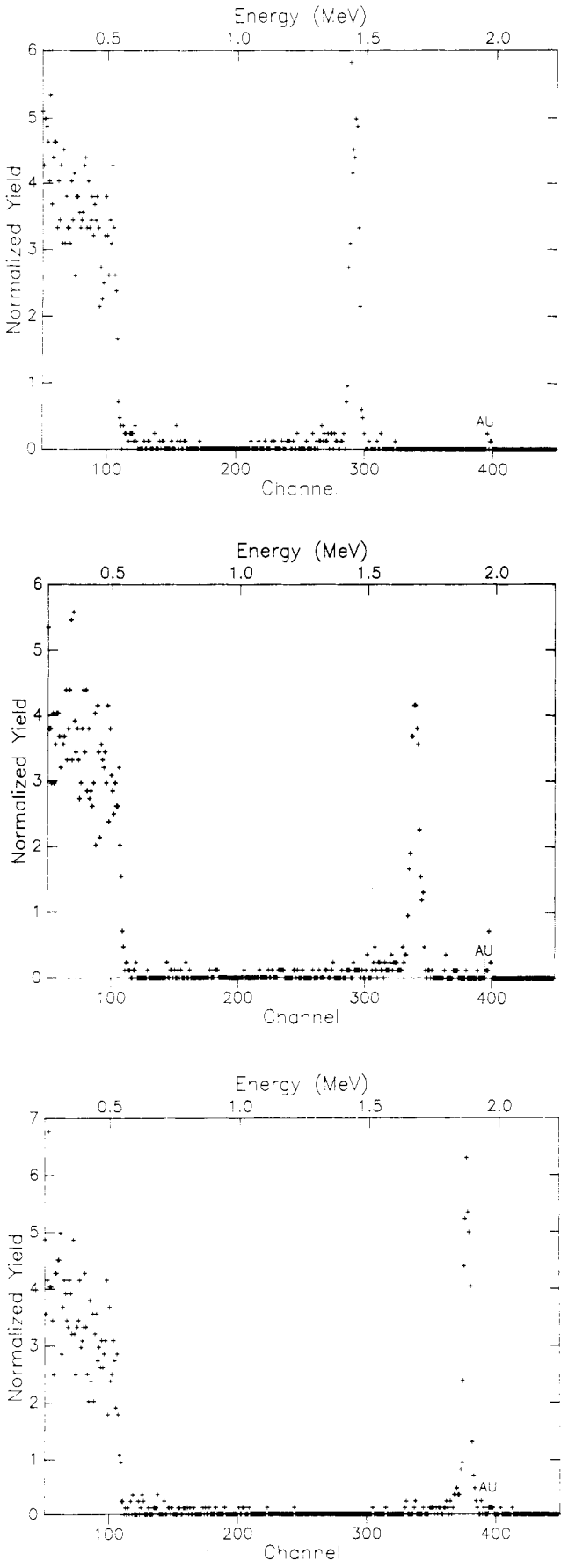

Figure 6. (a) Rutherford backscattering spectrum of PS/Au/PS sandwich before interdiffusion. (b) Rutherford backscattering spectrum after interdiffusion for 0.5 h at 174 °C. (c) Rutherford backscattering spectrum after 1.3 h at 174 °C. For this sandwich M of the top layer was 33 000 while M_D of the bottom layer was 2×10^7.

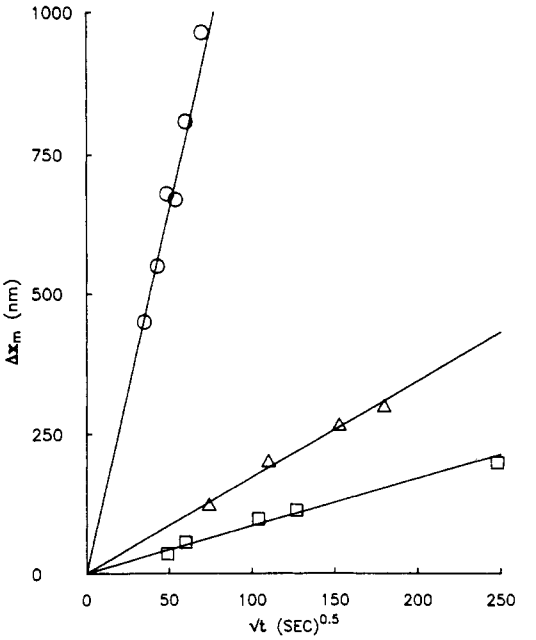

Figure 7. Gold marker displacement vs. square root of diffusion time at 174 °C for polystyrene. Circles are for M = 33 000, triangles for M = 254 000 and squares for M = 392 000 diffusing into polystyrene of $M_B = 2 \times 10^7$.

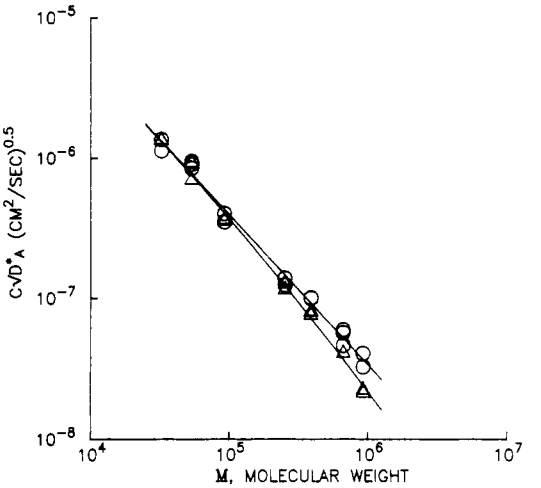

Figure 8. Slopes of marker displacement vs. square root diffusion time plots as a function of M, the molecular weight of the faster diffusing species. The circles are for data with PS bottom layers of 2×10^7 molecular weight while the triangles are for data with PS bottom layers of 1.8×10^6 molecular weight.

54 000, 93 000, 254 000, 390 000, 670 000, and 943 000 on top of a PS layer with $M_B = 2 \times 10^7$. The second series had the same set of top layers as the first but a bottom PS layer with $M_B = 1.8 \times 10^6$. Values of $C(D^*_A)^{0.5}$, from the slopes of Δx_m vs. $t^{0.5}$ plots, are displayed as a function of M in Figure 8 for both series of samples. Although the data for the lowest M's appear indistinguishable for both series, the $C(D^*_A)^{0.5}$ values for the lower M_B samples fall significantly below those for the high M_B samples as M approaches the former (1.8×10^6). This behavior is what one expects since as the molecular weights of the PS on either side of the Au markers approach each other, the net flux of matter past the markers decreases because V approaches 0 as D_A approaches D_B in eq 5. It is this effect that causes C to approach 0 in Figure 3 as N_A/N_B approaches 1. If this interpretation is correct the D^*_A's computed from Figure 8 using C from Figure 3 should be identical for both series of samples. The plot of D^*_A vs. M in Figure 9 shows exactly that result.

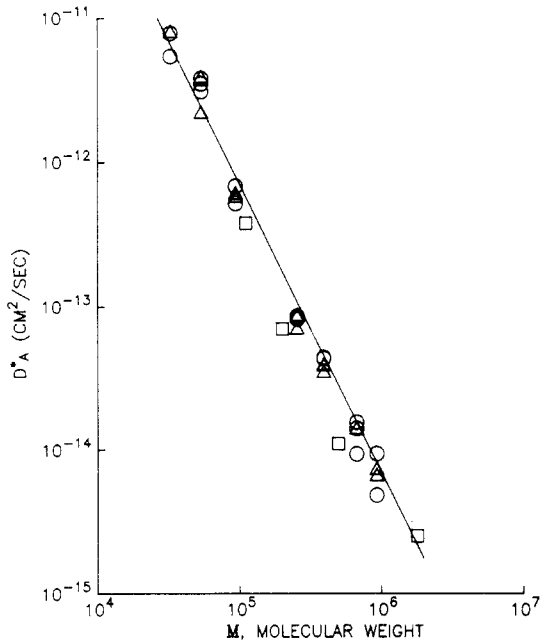

Figure 9. Self-diffusion coefficient D^*_A of polystyrene plotted against polymer molecular weight. The circles and triangles are extracted from the marker displacement data from the series with $M_B = 2 \times 10^7$ and $M_B = 1.8 \times 10^6$, respectively, at $T = 174$ °C. The squares are data obtained by Kumagai et al.[12] at 150 °C using a radiotracer technique.

Discussion

These marker displacement experiments show clearly that net mass flows (vacancy fluxes) occur during interdiffusion of polymers which have different molecular weights. While BJL have proposed that the marker displacements are due to their being dragged by the high molecular weight component in the broadening diffusion profile,[20] such an explanation is not possible if their assumption $J_A = -J_B$ holds. Since such drag must have its origins on the microscopic level in the frictional drag exerted by individual A and B segments on the boundary of the marker, the net frictional drag force on the marker must be zero if $J_A + J_B = 0$.

The molecular weight dependence of the marker displacement is also not consistent with that proposed by BJL.[20] They predict that Δx_m increases as $(D_0 t)^{0.5}$ where $D_0 = N_e B_0 k_B T/(N_A N_B)$. If that prediction were correct, the slopes of the Δx_m vs. $t^{0.5}$ plots should increase as $M^{-1}M_B^{-1}$. The data shown in Figure 8 increase much more strongly than M^{-1} and are practically independent of M_B except when M is not much less than M_B. The experimental results show that the assumption $J_A + J_B = 0$ does not accurately describe the interdiffusion of polymers in the melt.

We have made the alternative assumption that osmotic pressure gradients in the melt are relaxed rapidly enough that $\nabla \mu_v = 0$ at all times.[16,21] This assumption leads naturally to marker movement if D^*_A does not equal D^*_B. The fact that we measure the same D^*_A as a function of M for M_B's that differ by over an order of magnitude strongly suggests that this assumption, and the analysis that follows from it, are correct.

A least-squares fit to the data in Figures 9 reveals that

$$D^*_A = 0.007M^{-2.0\pm0.1}\ \text{cm}^2/\text{s} \qquad (17)$$

The exponent of M agrees with that predicted by the reptation theory. The order of magnitude of D^*_A also agrees with that expected from reptation. Graessley[22] has derived the following expression from the tube model of Doi and Edwards:[2,5]

$$D^*_A = (G_N^\circ/135)(\rho RT/G_N^\circ)^2 k_R (M_c/\eta_0(M_c))M^{-2} \qquad (18)$$

where G_N° is the shear modulus, and ρ the density of entangled chains, of the melt in the rubbery plateau region, R is the gas constant and $\eta_0(M_c)$ is the zero shear rate viscosity at the critical molecular weight M_c for the onset of entanglement. The constant k_R describes the mean square end-to-end distance R^2 of a molecule of mass M in the melt, i.e., $R^2 = k_R M$. In polystyrene $k_R = 5 \times 10^{-17}$ cm^2.[23] Substituting $G_N^\circ = 2 \times 10^6$ dyn/cm^2, $\rho = 0.96$ g/cm^3,[22] $M_c = 31\,000$, and $\eta_0(M_c) = 1200$ P[24] for polystyrene, we obtain

$$D^*_A = 0.006M^{-2}\ \text{cm}^2/\text{s} \qquad (19)$$

which agrees with the measured D^*_A, eq 17, to within a factor of 2.

Finally we can compare the D^*_A's extracted from the marker experiments with two other sets of measurements of D^*_A for monodisperse polystyrene. We have measured the diffusion of a 10–20-nm thick film of deuterated polystyrene into polystyrene using forward recoil spectrometry to profile the d-PS volume fraction as a function of depth.[25] These experiments in which ϕ of the d-PS is always less than 0.1 give

$$D^*_A = 0.008M^{-2}\ \text{cm}^2/\text{s} \qquad (20)$$

in excellent agreement with the marker movement result.

Kumagai et al.[12] have measured the interdiffusion of a thin (2–3 μm thick) film of monodisperse PS of molecular weight M into a thick film (30–40 μm thick) of monodisperse PS of molecular weight M_B using a radiotracer technique. If M is different from M_B we can now recognize that their analysis, which assumed a $\tilde{D}$ which was independent of composition, was incorrect. Since the radioactive decay of tritium measured depends markedly on the form of the $\phi(x,t)$ profile the $\tilde{D}$'s they extracted for the cases $M \ll M_B$ or $M \gg M_B$ are inaccurate[16] and may account for the fact that the M dependence they measured for D did not agree with the predictions of the reptation theory. However, for the case of $M = M_B$, i.e., self diffusion, D is constant and their analysis should be correct. Under these conditions $D^*_A = \tilde{D}$ so we have plotted their data (which were taken at 150 °C rather than 174 °C) in Figure 9. These D^*_A's agree both in magnitude and in slope with our preliminary marker data at 150 °C. These marker D^*_A's are decreased by a factor of about 2.2 from those measured at a diffusion temperature of 174 °C.

Conclusion

We have demonstrated that a net flux of matter occurs in concentrated diffusion couples of homopolymers where the polymers on either side of the couple have different intrinsic diffusion coefficients by virtue of their different molecular weights. The flux is toward the side which has the highest concentration of high molecular weight polymer, the slower moving species. This flux of matter can be measured by monitoring the displacement of markers placed at the initial interface. Very small fluxes can be measured by using Rutherford backscattering spectrometry. The marker displacements increase as $t^{0.5}$, as expected for diffusion fluxes. On the basis of numerical solutions to the diffusion equation the self-diffusion coefficient of the low molecular weight species can be extracted from the marker displacement data. The measured values of D^*_A decrease as M^{-2} in agreement with the predictions of the theory of reptation. The magnitudes of the D^*_A's are also in good accord with the theory as well as with values of D^*_A measured by other techniques.

Acknowledgment. The financial support of this research by the NSF-DMR Polymers Program under Grant DMR-8303174 is gratefully acknowledged. Peter Green received support in the form of a Public Health Service Pre-doctoral Fellowship. We also benefited from the use of the facilities of the Cornell Materials Science Center which is funded by the DMR-MRL program of NSF. We also thank F. Brochard, P.-G. de Gennes, H. H. Johnson, and D. N. Seidman for helpful discussions and correspondence on the diffusion aspects of this problem and D. Lilienfeld for assistance in programming the numerical solution to the concentration dependent diffusion equation.

Appendix A. Solution of the Diffusion Equation for Concentration-Dependent Polymer-Polymer Interdiffusion

To solve this diffusion problem eq 9 is first transformed to an initial value problem. A series of concentration profiles are then computed for the region to the right (Region 1) and to the left (Region 2) of the interface. This computation is done by choosing initial values of ϕ and ϕ' at $\eta = 0$ such that, in region 1 $\phi(+\infty) \rightarrow 0$, and in region 2 $\phi(-\infty) \rightarrow 1$. Curves of $\phi(0)$ vs. $\phi'(0)$ are then plotted for each region on the same graph and the intersection of these curves gives the unique pair of values $\phi(0)$ and $\phi'(0)$ which cause $\phi(-\infty) = 1$ and $\phi(+\infty) = 0$ to the simultaneously satisfied.

Region 1. We define a transformation variable S such that[26]

$$S \equiv \frac{\int_0^{\phi} \tilde{D}(\phi)\, d\phi}{\int_0^{\phi(0)} \tilde{D}(\phi)\, d\phi} \tag{A1}$$

which transforms eq 9 to the initial value problem

$$\frac{d^2S}{d\eta^2} = \frac{-2\eta}{\{1 - S[1 - (1 - \alpha\phi(0))^3]\}^{2/3}} \frac{dS}{d\eta} \tag{A2}$$

Equation A2 was solved by using the variable-order Adams predictor corrector method of integration subject to the following initial conditions:

$$S = 1 \qquad \text{at } \eta = 0 \tag{A3}$$

and

$$\left.\frac{dS}{d\eta}\right|_{\eta=0} = [3\alpha(1 - \alpha\phi(0))^2]\phi'(0)/[1 - (1 - \alpha\phi(0))^3] \tag{A4}$$

Region 2. We redefine S such that

$$S \equiv \frac{\int_{\phi}^{1} \tilde{D}(\phi)\, d\phi}{\int_{\phi(0)}^{1} \tilde{D}(\phi)\, d\phi} \tag{A5}$$

and thus eq 9 becomes

$$\frac{d^2S}{d\eta^2} = \frac{-2\eta}{\{(1 - \alpha)^3 + S[(1 - \alpha\phi(0))^3 - (1 - \alpha)^3]\}^{2/3}} \frac{dS}{d\eta} \tag{A6}$$

The initial conditions that must be satisfied are

$$S = 1 \qquad \text{at } \eta = 0 \tag{A7}$$

and

$$\left.\frac{dS}{d\eta}\right|_{\eta=0} = -[3\alpha(1 - \alpha\phi(0))^2]\phi'(0)/[(1 - \alpha\phi(0))^3 - (1 - \alpha)^3] \tag{A8}$$

Once the correct values of $\phi(0)$ and $\phi'(0)$ are found, the entire $\phi(\eta)$ curve may be computed from the corresponding $S(\eta)$ solutions. Selected results are shown in Figure 2.

References and Notes

(1) Graessley, W. W. *Adv. Polym. Sci.* **1974**, *16*, 1.
(2) Doi, M.; Edwards, S. F. *J. Chem. Soc., Faraday Trans. 2* **1978**, *8*, 1789, 1809, 1818.
(3) de Gennes, P.-G. *Macromolecules* **1976**, *9*, 587.
(4) de Gennes, P.-G. *J. Chem. Phys.* **1971**, *55*, 572.
(5) Edwards, S. F. In "Molecular Fluids"; Balain, R., Weill, G., Eds.; Gordon and Breach: New York, 1975; p 153.
(6) Klein, J. *Macromolecules* **1978**, *5*, 852.
(7) Klein, J. *Nature (London)* **1978**, *271*, 143.
(8) Klein, J.; Briscoe, C. *Proc. R. Soc. London, Ser. A* **1979**, *365*, 53.
(9) Klein, J.; Fletcher, D.; Fetters, L. J. *Nature (London)* **1983**, *304*, 526.
(10) Smith, B. A.; Samulski, E. T.; Yu, L.-P.; Winnik, M. A. *Phys. Rev. Lett.* **1984**, *52*, 1.
(11) Bartels, C. R.; Graessley, W. W.; Crist, B. *J. Polym. Sci., Polym. Lett. Ed.* **1983**, *21*, 495.
(12) Kumagai, Y.; Watanabe, H.; Miyasaka, K.; Hata, T. *J. Chem. Eng. Jpn.* **1979**, *12*, 1.
(13) Gilmore, P. T.; Falabella, R.; Lawrence, R. L. *Macromolecules* **1980**, *13*, 880.
(14) de Gennes, P.-G. *J. Chem. Phys.* **1980**, *72*, 4756.
(15) Klein, J. *Macromolecules* **1981**, *14*, 480.
(16) Kramer, E. J.; Green, P. F.; Palmstrom, C. J. *Polymer* **1984**, *25*, 473.
(17) Crank, J. "The Mathematics of Diffusion", 2nd ed.; Oxford University Press: Oxford, UK., 1975; pp 203–214.
(18) Brochard, F.; Jouffroy, J.; Levinson, P. *Macromolecules* **1983**, *16*, 1638.
(19) Chu, W. K.; Mayer, J. W.; Nicolet, M. A. "Backscattering Spectrometry"; Academic Press: New York, 1978; p 1.
(20) Brochard, F.; Jouffroy, J.; Levinson, P. *J. Phys. (Paris), Lett.*, to be published.
(21) The assumption $\nabla\mu_v = 0$ effectively denies any coupling between the center-of-mass diffusion of chains and chain relaxation. (Chain relaxation is much faster than chain diffusion.) While this assumption seems to be correct in the melt, it is almost surely incorrect in the glass, even for small-molecular diffusing species. The coupling in the latter case gives rise to extreme non-Fickian, case II, diffusion.
(22) Graessley, W. W. *J. Polym. Sci., Polym. Phys. Ed.* **1980**, *18*, 27.
(23) Kurata, M.; Tsunashima, Y.; Iwama, M.; Kamada, K. In "Polymer Handbook", 2nd ed.; Brandrup, J., Immergut, E. H., Eds.; Wiley: New York, 1975; p IV-40.
(24) Graessley, W. W.; Roovers, J. *Macromolecules* **1979**, *12*, 959.
(25) Mills, P. J.; Green. P. F.; Palmstrom, C. J.; Mayer, J. W.; Kramer, E. J., submitted for publication.
(26) Lee, C. F. *J. Inst. Math. Appl.* **1972**, *10*, 129.
(27) Tirrell, M. *Rubber Chem. Technol.* **1984**, *57*, 523.